

Proximity-induced superconductivity in a narrow metallic wire

H. Courtois,* Ph. Gandit, and B. Pannetier

*Centre de Recherches sur les Très Basses Températures, CNRS (Associé à l'Université Joseph Fourier),
25 Avenue des Martyrs, Grenoble, France*

(Received 21 February 1995; revised manuscript received 11 April 1995)

We present a study of the superconducting proximity effect on electron transport in hybrid metallic nanostructures. The effects of barrier transparency and geometrical confinement in lateral structures are compared. In a long narrow metallic (N) wire in contact with small superconducting (S) islands through mesoscopic normal-superconductor (N - S) junctions, a zero-resistance state is obtained. Experimental behavior diverge to a large extent from the classical models. Critical-current measurements are reported that show an anomalous amplitude and a nonconventional temperature dependence behavior.

Electron-transport properties of normal-metal-superconductor (N - S) junctions have very recently raised considerable interest funded by significant experimental deviations from the classical models.¹ Most of these intriguing properties are now believed to be related to multiple Andreev reflections of normal electrons at the superconducting interface.^{2,3} Andreev reflection is the microscopic mechanism of proximity effect and electronic current conversion, in which one electron coming from N is reflected as a coherent hole, while a Cooper pair is transmitted in S . This process takes place in S over a distance equal to the superconducting coherence length ξ_S . Electron-reflected-hole coherence leads to coherent addition of electron transmission probability amplitudes, which enhances significantly total conductance through the N - S junction compared to the classical result. Hekking and Nazarov calculated the low-temperature ($k_B T \ll \Delta$) conductance of a N - N' - S junction,⁴ disorder being restricted to the normal region N' of resistance r . Electron confinement in N' near the S interface was shown to induce a finite subgap resistance R_I of order R_T^2/r , R_T being the tunnel resistance of the N' - S interface. If the S electrode is split in two electrodes with different superconducting phases, interferences occur between Andreev currents.⁵

Very recently, Zhou, Spivak, and Zyuzin calculated the spatial dependence of the electric field in the vicinity of a disordered N - S junction,⁶ introducing the barrier-equivalent length $L_t = l_e/t_0$, which is the length of N metal having a resistance R_T . The dimensionless transmission coefficient t_0 (≤ 1) gives the transmission probability through the N - S interface, whereas l_e is the elastic mean free path in N . The resistance R_I of the N - S junction then has the simple form

$$R_I = \gamma R_T \frac{L_t}{L_T}, \quad (1)$$

where γ is a numerical factor of order 1. The normal coherence length L_T is the decay length of the proximity-induced pair amplitude in N . Evaporated metals are in the dirty limit, where $l_e < L_T$ and $L_T = \sqrt{\hbar D / 2\pi k_B T}$, D being the electronic diffusion

length. Relation (1) is similar to the result of Hekking and Nazarov if N' is taken as a length L_T of metal N . This shows the direct influence of the transport properties of N on the conductance of a N - S junction. In this context, the properties of a normal metal N in the vicinity of a S interface have not been directly investigated yet. Here, we report measurements of transport in the N part of hybrid metallic nanostructures that provide a new insight in proximity effect at the mesoscopic scale.

We fabricated normal metal ($N = \text{Cu}$ or Ag) nanostructures in clean metallic contact with submicrometer superconducting islands ($S = \text{Al}$). Most of the samples discussed here are made of a narrow N wire forming N - S nanojunctions with an array of lateral S islands, see Fig. 1. The total length is $76.8 \mu\text{m}$, whereas the cell parameter d is between 0.4 and $2.5 \mu\text{m}$. The widths $w_{N,S}$ and thicknesses $e_{N,S}$ of the N, S wires are of order 100 nm . The fabrication technique by two-axes shadow evaporation has been described elsewhere.⁷ Oblique metallic evaporations were performed in a ultrahigh vacuum (UHV) chamber on a PMMA resist mask suspended 500 nm above the Si substrate. During the same vacuum cycle, N and S structures were evaporated with the same angle of 45° to the substrate plane, but along perpendicular axes. The pressure during the whole process never exceeds $2 \times 10^{-8} \text{ mbar}$, which ensured us of a high-quality interface between the two metals. A different technique has been used for nanofabricating single Cu loops with two Al electrodes.⁸ Both structures were patterned by two successive lift-off lithographies, the surface of Cu being cleaned by accelerated (500 V) Ar ions for 20 s , just before Al evaporation in the same vacuum ($P \approx 10^{-6} \text{ mbar}$).

We performed transport measurements in a μ -metal shielded dilution refrigerator down to 30 mK . In all the experiments, electron current is flowing along the continuous N wire, but not through the N - S interface. The main advantage of the long wire geometry is that the transport measurement is greatly sensitive to the proximity effect in N , but not to any boundary effect for instance related to electronic current conversion. We carefully designed in-line contacts in order to reject measurement artifacts occurring at the superconducting transition of the contacts, due to current redistribution in the sample.⁹

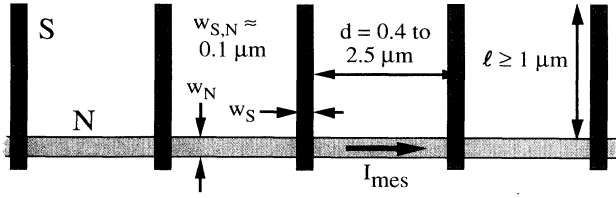


FIG. 1. Geometry of a part of a sample. A narrow metallic ($N = \text{Cu}$ or Ag) wire constitutes submicrometer N - S junctions with a 1D array of superconducting ($S = \text{Al}$) islands. The cell parameter d of the array is 0.4 to 2.5 μm , the width of the wires is about 100 nm, and the length of the S islands is more than 1 μm . Measurement current I_{mes} flows along the continuous N wire.

High attenuation lithographed high-frequency filters¹⁰ were integrated at low temperature in the sample holder.

Figure 2 shows the behavior of the resistance R of three samples, normalized to the normal-state value R_n , in the vicinity of Al superconducting transition temperature T_c . Samples 15 and 17 are long wires, respectively, made of Cu and Ag, with Al islands in contact, the cell parameter d being 0.8 μm . Sample 18 is a mesoscopic Cu loop of diameter 500 nm with two 1 μm apart Al islands, the distance between electrical contacts being 1.5 μm . Electron mean free path l_e values range from 5 to 57 nm, see Table I. The measured resistance of samples 17 and 18 shows some structure at $T_c \approx 1.4$ K, which is near the critical temperature of bulk Al. This shows that the critical temperature of Al is not significantly depressed by inverse proximity effect, which is consistent with the large length l ($\geq 1 \mu\text{m}$) of the Al strips compared to the superconducting coherence length ξ_S (≈ 100 nm).¹¹ Below T_c , samples 17 and 18 show a sharp decrease of the resistance, while the resistance decrease in sample 15 is unobservable at the scale of Fig. 2. The relative amplitude of the resistance decrease in samples 17 and 18 (11 and 19 %, respectively) approximately corresponds to the ratio w_S/d of N wire length covered by the S film (15 and 23 %). This leads to the intuitive interpretation that the N wire is locally shorted by the S strip. The different behaviors are interpreted by the presence or not of a barrier at the N - S interface, which can decouple the N wire from the S island.

Near T_c , the normal coherence length L_T is smaller than d , so that each N - S junction can be considered as decoupled from its neighbors. Let us consider the contribution $R_{N/S}$ of the N - S overlap region of length w_S to the resistance of the N wire. In this region, the resistance

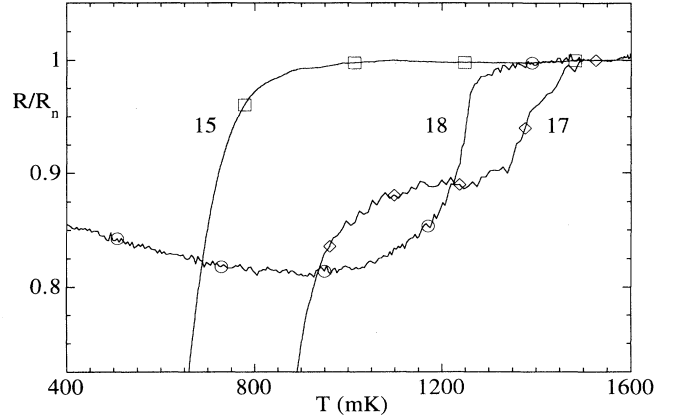


FIG. 2. Temperature dependence of the resistance R of samples 15, 17, and 18, normalized to the normal-state resistance R_n . The Al superconducting transition is $T_c = 1.4$ K. Measurement current is 50 nA. See Table I for parameters values.

R_N of the N wire segment, and R_S of the S strip in its width, act as parallel resistances with distributed coupling through the temperature-dependent barrier resistance R_I . Deviation of $R_{N/S}$ from its normal-state value provide precise information on the barrier through direct comparison of the barrier-equivalent length L_t with the geometrical length w_S^2/e_N which takes into account the confinement in N below the S interface. In the low transparency case, the barrier resistance at T_c , $R_I(T_c) = R_T$, is much larger than R_N which gives the condition $L_t > w_S^2/e_N$. Superconductivity in S ($R_S = 0$) then has little effect on the resistance $R_{N/S}$, which decreases very slowly below T_c thanks to residual proximity effect in N . Sample 15 fits in this category, with a L_t , deduced from a complete analysis⁶ of order 3 μm , R_T being of order 1 Ω . This barrier is presumably due to a disordered region at the Cu/Al interface created by room-temperature interdiffusion. Comparison of the residual resistivity ratio of single layers and a bilayer of Cu and Al showed that this diffusion is restricted to a thickness of about 50 \AA .

In the opposite limit of high transparency at the N - S interface ($L_t < w_S^2/e_N$), the resistive transition of S effectively shorts the N piece in contact, so that the resistance $R_{N/S}$ is near zero below T_c . Samples 18 and 17 belong to this latter category, with a resistance drop ΔR of the order of $R_{N/S}(T > T_c)$, but a different low-temperature behavior. Sample 17 resistance continues to

TABLE I. Characteristic parameters of different samples.

Sample	w_N (nm)	w_S (nm)	e_N (nm)	d (μm)	r_n (Ω)	l_e (nm)	$L_T\sqrt{T}$ (μm)	$L_T^{\text{fit}}T$ (nm)	$r_n I_c$ (0 K) (nV)
13 (Cu)	240	100	150	0.4	0.25	30	0.14	24.2	225
14 (Cu)	220	120	150	1.6	1.05	32	0.14	61.6	222
15 (Cu)	220	120	155	0.8	0.28	57	0.19	67.6	185
17 (Ag)	210	120	150	0.8	0.66	33	0.14	69.3	1698
18 (Cu)	50	175	30	1.5	103	5.1	0.057	39.8	1940

decrease at low temperature, in the expected way for an increasing proximity effect. Following Eq. (1), this Ag/Al sample then verifies $L_t < \min[w_S^2/e_N, L_T(T_c)] = 0.1 \mu\text{m}$, which leads to $R_T < 0.1 \Omega$ and $t_0 > 28\%$. This remarkable transmission coefficient demonstrates the high quality of the N - S interface our *in situ* process. On the contrary, sample 18 resistance shows a nonmonotonous behavior that can be accounted for by an intermediate barrier strength, so that $L_t > L_T$. Following Eq. (1), the barrier resistance R_I is in this case relatively small at T_c , but increases at lower temperature. The coexistence of the resistance drop at T_c and the increase below give the condition $w_S^2/e_N > L_t > L_T$, which leads to a barrier resistance obeying $20 > R_T > 1.8 \Omega$. This relatively large interface resistance is due to the imperfection of the Cu surface cleaning procedure and the lower quality of the vacuum.

The comparison of samples 17 and 18 shows that both a high transparency of the barrier (sample 17), or a strong confinement in N , for example due to small N -layer thickness compared to junction size, (sample 18) have a comparable effect on transport through a N - S junction. A given value of interface resistance may give different behavior of transport in the vicinity of a N - S junction, depending on the electron diffusivity in N . This is precisely the effect of confinement by the disorder on the subgap transmission of the N - S junction.⁴ As a first result, we therefore observe a behavior at the transition that is qualitatively accounted for in the framework of the theory of Zhou *et al.*⁶

At this stage, it is worth noting that Lambert, Hui, and Robinson have calculated the susceptibility of a N -metal conductance to the presence of a superconducting order parameter in a S inclusion.¹² This quantity was found to be either positive or negative, depending on the disorder realization. Indication of such mesoscopic anomaly was reported in previous works on hybrid systems similar to ours but with shorter total lengths.¹³ In contrast, we did not observe any increase of resistance above the normal-state value, nor fluctuations of the conductance susceptibility. Although these mesoscopic effects should be washed out by ensemble average in long wires (samples 15 and 17), they should remain in the mesoscopic loops (sample 18 and other similar samples).

At low temperature, the coherence length L_T becomes of the order of the distance d and a zero-resistance state occurs. Let us emphasize that the occurrence of a zero-resistance state in the N wire must not be confused with conventional Josephson effect in proximity junctions (S - N - S). Here we are considering a long N wire where superconductivity is locally injected by multiple N - S nanojunctions. Figure 3 shows the current-differential resistance characteristic of sample 17 at 150 mK, which clearly exhibits a sharp $1.76 \mu\text{A}$ critical current. This characteristic deviates significantly from the classical resistively shunted junction (RSJ) model for a S - N - S junction between two bulk superconductors. In this respect, the sharpness of the differential resistance increase is not consistent with the relatively small magnitude of the peak. In a crude view, this system could be seen as a one-dimensional (1D) array of S' - N - S' junc-

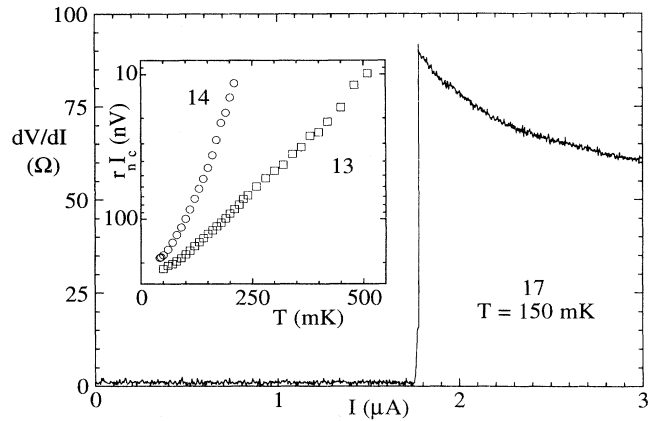


FIG. 3. Current-differential resistance characteristic of Ag/Al sample 17 at $T=150 \text{ mK}$. Normal-state resistance is $R_n=63.3 \Omega$, and measurement current is 10 nA . The critical current is $1.76 \mu\text{A}$. Inset: Product of the one cell normal-state resistance r_n with the critical current I_c for Cu-Al samples 13 and 14, of respective cell parameter $d=0.4$ and $1.6 \mu\text{m}$, in inverse logarithmic scale. Linear behavior accounts for a $\exp(-T/T^*)$ temperature dependence for the critical current.

tions, S' being the N metal region in close contact with S . de Gennes calculated the critical current I_c of a macroscopic S - N - S junction:¹¹

$$r_n I_c = \frac{\pi \Delta}{2e} \frac{L/L_T}{\text{sh}(L/L_T)}, \quad (2)$$

where Δ is the gap in the S' electrodes at the interface and $L=d-w_S$ is the length of the junction. Equation (2) is derived from the Ginzburg-Landau theory, so that strictly speaking it is valid only near T_c . Here, the small amplitude of the pair amplitude induced in N by proximity effect validates its use even at very low temperature.

We measured the critical current of a variety of samples as a function of temperature with a differential resistance criteria of $0.1R_n$. The inset of Fig. 3 shows the measured $r_n I_c$ product of the critical current I_c with the normal-state resistance of one cell r_n for samples 13 and 14. These Cu/Al samples of respective cell parameter 0.4 and $1.6 \mu\text{m}$ were coevaporated on the same substrate. At high temperature, the thermal rounding of the current-voltage characteristics prevents accurate measurement of the critical current. In the high-temperature limit ($L_T \ll L$), Eq. (2) can be approximated by an exponentially decaying law. The inverse logarithmic plot of the inset of Fig. 3 then qualitatively shows the temperature dependence of $1/L_T$. The linear temperature dependence of the two curves indicates a $1/T$ temperature dependence of L_T . This behavior is characteristic of a clean limit, where the mean free path l_e is larger than the coherence length $L_T = \hbar v_F / 2\pi k_B T$, v_F being the Fermi velocity.

Figure 4 shows the measured critical current of sample 17 together with two fits following (2) in a clean or dirty regime for L_T temperature dependence. We assumed a temperature-independent gap Δ . One can readily see that

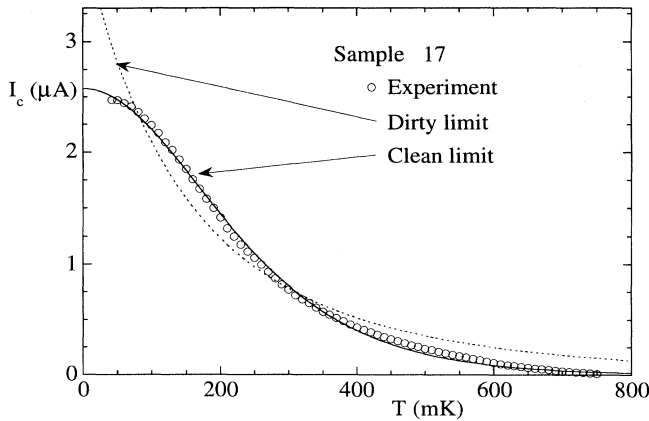


FIG. 4. Temperature dependence of the critical current of sample 17 in parallel with clean- and dirty-limit fits to theory. Clean-limit law ($L_T \propto 1/T$) shows an excellent agreement to the data, contrarily to the expected dirty-limit ($L_T \propto 1/\sqrt{T}$) fit. The effective coherence length is $L_T^{\text{fit}} = 69.3 \text{ nm}/T \text{ (K)}$ and the zero-temperature $r_n I_c$ product is $1.7 \mu\text{V}$.

the dirty-limit fit has a very poor agreement with the data, especially at low temperature, where the saturation of the critical current is not described. On the contrary, the clean-limit fit shows a surprisingly good agreement with the data in the whole temperature range. This result is definitely unconventional by contradicting the classical criterion between clean and dirty regime of the coherence length. This criterion would indicate here a dirty limit since the mean free path ($l_e = 33 \text{ nm}$ in sample 17) is much smaller than the coherence length L_T at every temperature. Nevertheless, the best fit value $L_T^{\text{fit}} = 69.3 \text{ nm}/T \text{ (K)}$ is more than one order of magnitude smaller than the predicted length in the clean limit ($1.68 \mu\text{m}$ at 1 K). The dirty-limit expected value is $0.14 \mu\text{m}/\sqrt{T \text{ (K)}}$. We observed this same behavior with very close experimental values in more than ten Cu/Al and Ag/Al samples with various interface transparencies. Table I lists the parameters derived from the experimental data of different samples. We checked that taking another criteria for the determination of the critical current, as the position of the differential resistance maximum, had no influence on these results. Similar anomalous behavior has been previously reported in magnetization measurements of Nb/Cu and Nb/Ag coaxial wires by Mota, Marek, and Weber.¹⁴ A pure clean-limit behavior was found for a L_T/l_p ratio up to 80, which is close to ours. In contrast with the results of Mota, Marek, and Weber, the fact that we experimentally do not find the right Fermi velocity throws some doubt on a simple interpretation in terms of a plain clean regime.

Another striking result concerns the amplitude of the low-temperature critical current. The fit-derived $r_n I_c$ ($T = 0 \text{ K}$) product of sample 17 is $1.7 \mu\text{V}$, which is much smaller than the theoretical value $\pi\Delta_{\text{Al}}/2e = 530 \mu\text{V}$ derived from the bulk Al gap. An interpretation in terms of barrier transparency is unlikely, because of the highly transparent N - S interface of this particular sample (17). Samples with a low transparency interface, like sample 15, even show a $r_n I_c$ product ($= 0.19 \mu\text{V}$ for sample 15) little depressed compared to sample 17, as if the interface transparency would have only a small effect on the critical current.

The huge discrepancy between existing theories and experiment shows that this system definitely cannot be described by classical models, even in an anomalously clean regime or in a barrier-dominant regime. Taking into account the array geometry does not modify this conclusion either. The main difference of this system compared to classical ones is clearly that the superconducting islands are neither in-line or massive like they are in a conventional S - N - S junction. The question of conversion from normal electronic current to supercurrent is considerably less straightforward in this lateral geometry, and one can wonder whether electrons in N are sensitive or not to the order parameter in the superconductor S in contact. For instance, the proximity-induced critical current in N should rather be linked to the induced superconducting properties in N . The small amplitude of the measured critical current can then be related to the small order of magnitude of the proximity-induced energy gap in N .^{6,15} In a normal metal in the vicinity of a superconducting interface, the density of states can be close to zero for small energies, even if the electron interaction is zero.

In summary, we presented electron-transport investigation of the proximity effect in a narrow metallic wire. Below T_c , both the electron confinement in N and the nonideal transparency of the N - S interfaces are needed to describe the various experimental situations. The study of the low-temperature zero-resistance state shows a purely new behavior, that is definitely out of the scope of classical S - N - S junctions models. This system exhibits a weak, but long-range superconducting state with promising features with respect to the mesoscopic regime where fluctuations of charge and electron-wave interference become relevant.^{16,17}

We thank L. Dumoulin, P. Martinoli, B. Spivak, A. Volkov, and F. Zhou for stimulating discussions and D. Maily for fabricating sample 18. This work is supported by European Community through the "Supnet" network, Contract No. CHRX-CT92-0068.

*Present address: Institut de Physique de l'Université de Neuchâtel, 2000 Neuchâtel, Suisse.

¹A. Kastalsky, A. W. Kleinsasser, L. H. Greene, R. Bhat, F. P. Milliken, and J. P. Harbison, Phys. Rev. Lett. **67**, 3026 (1991).

²B. J. van Wees, P. de Vries, P. Magnée, and T. M. Klapwijk,

Phys. Rev. Lett. **69**, 510 (1992).

³I. K. Marmokos, C. W. J. Beenakker, and R. A. Jalabert, Phys. Rev. B **48**, 2811 (1993).

⁴F. W. J. Hekking and Yu. V. Nazarov, Phys. Rev. Lett. **71**, 1625 (1993); Phys. Rev. B **49**, 6847 (1994).

- ⁵H. Pothier, S. Guéron, D. Estève, and M. H. Dévoret, *Phys. Rev. Lett.* **73**, 2488 (1994).
- ⁶F. Zhou, B. Spivak, and A. Zyuzin, *Phys. Rev. B* (to be published).
- ⁷H. Courtois, Ph. Gandit, and B. Pannetier, *Phys. Rev. B* **51**, 9360 (1995).
- ⁸H. Courtois, Ph. Gandit, D. Mailly, and B. Pannetier (unpublished).
- ⁹H. Courtois, Ph. Gandit, and B. Pannetier (unpublished).
- ¹⁰H. Courtois, O. Buisson, J. Chaussy, and B. Pannetier, *Rev. Sci. Instrum.* **66**, 3465 (1995).
- ¹¹P. G. de Gennes, *Rev. Mod. Phys.* **36**, 225 (1964).
- ¹²C. J. Lambert, V. C. Hui, and S. J. Robinson, *J. Phys. Condens. Matter* **5**, 4187 (1993).
- ¹³V. T. Petrashov, V. N. Antonov, S. V. Maksimov, and R. Sh. Shaidorov, *JETP Lett.* **58**, 49 (1993).
- ¹⁴A. C. Mota, D. Marek, and J. C. Weber, *Helv. Phys. Acta* **55**, 647 (1982).
- ¹⁵A. F. Volkov, *Phys. Lett. A* **187**, 404 (1994).
- ¹⁶V. T. Petrashov, V. N. Antonov, P. Delsing, and R. Claeson, *Phys. Rev. Lett.* **70**, 347 (1993).
- ¹⁷R. Fazio, C. Bruder, and G. Schön, *Physica B* **203**, 247 (1995).

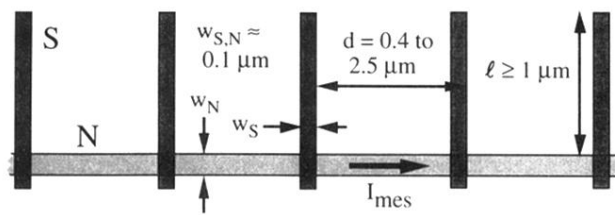


FIG. 1. Geometry of a part of a sample. A narrow metallic ($N = \text{Cu}$ or Ag) wire constitutes submicrometer N - S junctions with a 1D array of superconducting ($S = \text{Al}$) islands. The cell parameter d of the array is 0.4 to $2.5 \mu\text{m}$, the width of the wires is about 100 nm , and the length of the S islands is more than $1 \mu\text{m}$. Measurement current I_{mes} flows along the continuous N wire.